ISSN 2176-5480

22nd International Congress of Mechanical Engineering (COBEM 2013)
November 3-7, 2013, Ribeirão Preto, SP, Brazil

DESIGN AND MANUFACTURE OF MICROCHANNEL HEAT SINKS FOR HIGH CONCENTRATION PHOTOVOLTAIC CELLS

Correa, Marco [1]; marcoalves@ufrj.br
Guerrieri, Daduí Cordeiro [2]; guerrieri@cefet-rj.br
Naveira-Cotta, Carolina Palma [1], carolina@mecanica.coppe.ufrj.br
Colman, Jordana [1]; jordanacolman@yahoo.com.br

[1] – Laboratory of Nano and Microfluidics and Micro-Sistems - LabMEMS, Mechanical Eng.Dept. - POLI & COPPE/UFRJ, Rio de Janeiro, Brazil
[2] – Mechanical Engineering Coordination - CEFET-RJ, Itaguaí, Brazil

Abstract. *This paper presents the optimized design, fabrication and experimental analysis of a heat sink based on microchannels for efficient cooling of a commercial high concentration photovoltaic (HCPV) cell. The optimized geometry of the heat sink was made using the platform ANSYS program Workbench 14.5 CFX and optimization tool Response Surface optimization, based on some requirements and design limitations such as: the mean temperature and standard deviation on the solar cell, the average fluid temperature at the micro-heat sink outlet and maximum temperature in the fluid domain. The optimized heat sink was manufactured in copper using a CNC-micro milling machine and an experimental setup was assembled to analysis the micro-heat exchanger first in laboratory conditions.*

Keywords: *micro-heat sink, high concentration photovoltaic cell, HCPV, optimization, micro-milling, experimental analyses*

1. INTRODUCTION

After more than five decades of research and development, the photovoltaic's areas is recently growing rapidly. Its main advantage is the abundance of solar energy, which provides opportunities for the development of sustainable technologies for electricity generation. The use of photovoltaic cells with high concentration systems (HCPV) minimizes the need of very expensive cells, thereby reducing the capital required with big silicon substrates by using a low cost optical elements. High concentration systems has allowed the more recent solar technologies competing with other energy approach.

However, most of the solar energy incident in a photovoltaic systems is wasted as heat, leading to unwanted increase of the temperature on the solar cell which consequently leads to a reduction of efficiency. In this sense the cooling systems of these cells has a major technological importance in this research area, aiming to increase their efficiency and thus preventing the degradation of the cells with excessive temperature. The uniformity of temperature on the solar cell is another important parameter that affects its efficiency. These aspects require careful control and optimized heat dissipation system for high concentration photovoltaic cells, and it is in this context that the present paper is inserted.

According to HO *et al.* [1] the photovoltaic cells became highly popular because they are considered cleaner compared to fossil fuels. However, this kind of conversion into electrical energy is still considered expensive compared to others. To reduce costs, HO *et al.* still claim that the use of lenses or mirrors decreases the cost of cell concentrators because it demands fewer cells, hence less silicon is required. According to HO *et al* [1], the efficiency of PV cells is around 25%, where it reaches its current limit. A great part of solar energy is converted into thermal energy which must be removed from the cell to avoid excessive temperature rise. The article even states that in the energy balance of a natural convection cooled PV cell with 100 suns concentration, the cell can reach temperatures as high as 1200 K.

In [2] – another article from HO *et al.* – it's been studied the impact caused by the cooling of the cells in the solar concentration limit. The authors state that for a heat sink with heat transfer coefficient on the order of:10^6 W m^{-2} K^{-1}, the maximum possible concentration is on the order of 10,000 suns: i.e. 10^7 W m^{-2}. At such a high heat flux, the thermal conductivity of the cell becomes the dominant factor in the heat removal efficiency. HO *et al* .[2] claim that, in practice, the solar concentration varies between 10 and 1000 suns and above 4 suns a more efficient cooling devices is needed than only a natural convection and radiation across the surface of the cell.

ROYNE *et al* .[3] studied the photovoltaic cell cooling under solar concentration. They claim that a single cell PV needs only a passive cooling system, but for *arrays* of concentrations above 150 suns, it becomes necessary to use an active system with heat resistance lower than 10^{-4} m^2 K W^{-1}. Only a fraction – around 25% – of the solar energy is converted into electrical energy and the remaining energy is converted into thermal energy.

SALA [4], MBEWE *et al.*[5] and DALAL & MOORE [6] showed that the PV cell efficiency linearly dependent on its temperature. In their articles the authors reported that the efficiency decreases with increasing temperature. The manufacturer SunPower points in [7] that high temperatures could cause damage to cells, decrease its efficiency and life span. SANDERSON *et al.*[8] states that the non-uniformity of temperature throughout the cell also contributes to the decrease of its efficiency. KERMANI [9] states that the non-uniformity and hot sposts casued by lenses and mirrors also contributes to decrease cell efficiency.

ISSN 2176-5480

Pioneeringly, TUCKERMAN and PEASE [10] studied in 1981 the intensification of heat exchange in microchannel heat sinks for electronic devices of high thermal dissipation. At that time, the so-called VLSI circuits (*Very-large-scale integrated*) could dissipate up to 100 W in small areas. It was believed that the physical limit for heat sinks was on the order of 2 x 10^5 W m^{-2}. Using microchannels, the authors showed that it would be possible to dissipate heat fluxes as high as 10^7 W m^{-2}. In addition, they have experimentally demonstrated a cooling device with a maximum thermal resistance of 9 x 10^{-6} m^2 K W^{-1}, and have found that for heat fluxes of 7.9 x 10^6 W m^{-2}, a maximum temperature difference between the substrate and the fluid inlet temperature is 71 K.

DANG and TENG [12] conducted a theoretical-experimental comparative study to evaluate the relationship between the thermal exchange efficiency and pressure drop in mini and micro channels. Three aluminum heat exchangers were studied by varying width, height, and number of channels. The heat exchanger of 500 μm wide by 2000 μm high is between 1.2 and 1.32 times more effective than 1000 μm x 250 μm; and between 1.5 and 1.53 times more effective that the 2000 μm x 250 μm. However, the pressure drop is always greater in smaller hydraulic diameter, which demands a greater pumping power. Before carrying out the experiments, the authors studied the heat exchangers using COMSOL Multiphysics and obtained consistent results.

From the above studies it is possible to perceive the need to find the optimal geometry that maximizes the heat exchange and minimize energy expenditures for a given problem. In this sense, HUSAIN and KIM [13] proposed a numerical study of optimization with the help of finite volume program ANSYS CFX 11.0. The authors constructed a polynomial response surface by correlating the input variables to the objective functions. These functions are minimized using an evolutionary algorithm.

ESCHER *et al.* [14] claim that the precursor model proposed by TUCKERMAN and PEASE [10] although simple, has some disadvantages that should be corrected in order to obtain a high performance heat exchanger. The largest of these is the long path traveled by the fluid, which results in non-uniform temperature on the substrate and high pressure drop. They propose that these disadvantages can be minimized if the path of the fluid is divided into numerous smaller pieces and fed from a manifold located in a layer above resulting in impingement jet. The authors proposed a 3D model to study the influence of geometric parameters on the thermal and hydrodynamic performance of the heatsink. Then, from the 3D model, a semi-empirical model was carried out. The optimized model was able to dissipate 7.5 x 10^6 W m^{-2} keeping a temperature difference between the substrate and the fluid at the entrance of 65 K. The necessary flow rate was 1 liter per minute resulting in a pressure drop as low as 0.1 bar.

In this sense, the present study aims to a optimal design, fabrication and experimental analyses of a micro channel heat sink for efficient cooling of high concentration photovoltaic cells (HCPV). The design was based on the use of commercial cells for high concentrations from Spectrolab, a subsidiary of Boeing, supposing the solar incidence of Rio de Janeiro region for the thermal load calculation on the HCPV cell.

Based on certain requirements and limitations of the project, such as the mean temperature and standard deviation on the solar cell, the average fluid temperature at the micro-sink outlet and maximum temperature in the fluid domain, the present work performed the optimization of the geometric and flow rate parameters in ANSYS Workbench 14.5 via CFX and Response Surface Optimization tool. The optimized micro heat sink was fabricated in copper using a micro milling CNC. The experimental setup was assembled specially for this work, and three different test cases of the manufactured micro heat sink are carefully presented here.

2. HEAT SINK PROJECT

As was called the attention on the literature review, some works states that the efficiency of the photovoltaic cell is inversely proportional to the temperature of the solar cell. In other words: as much as the solar energy contributes to the electricity generation, as higher it is the cell temperature and consequently lower is its efficiency.

This work was developed taking into account a HCPV cell from Spectrolab-Boing, model 100 CCA C3MJ 1 Concentrator Cell Assembly [15] who owns a cell silicon triple junction assembled on a ceramic substrate and with a theoretical efficiency of 38.5%, as presented in Fig. 1. In Figure 1 we can also see the dimensional details of the silicon cell (in black in the center) placed over a ceramic substrate (yellow) which is used to connect the power cables. The solar cell has dimensions of 9.85 mm x 9.89 and the whole substrate has 21 x 25.5 mm.

Above the photovoltaic cell is placed a set of lenses and mirrors to amplify and focus the solar radiation, as shown in the schematic draw presented in Figure 2. For this project it was assumed that the lens systems was capable to concentrate 1000 times the sun energy.

According to data from SWERA of the American organ NREL, considering the maximum solar energy radiated during the summer in Rio de Janeiro, in the month of January among 11 to 12 am, the total irradiance can be considered as 600 W / m². Therefore, the radiation incident on the cell, used in the thermal analyses by this work, was in the order of 6 x 10^5 W/m^2.

ISSN 2176-5480

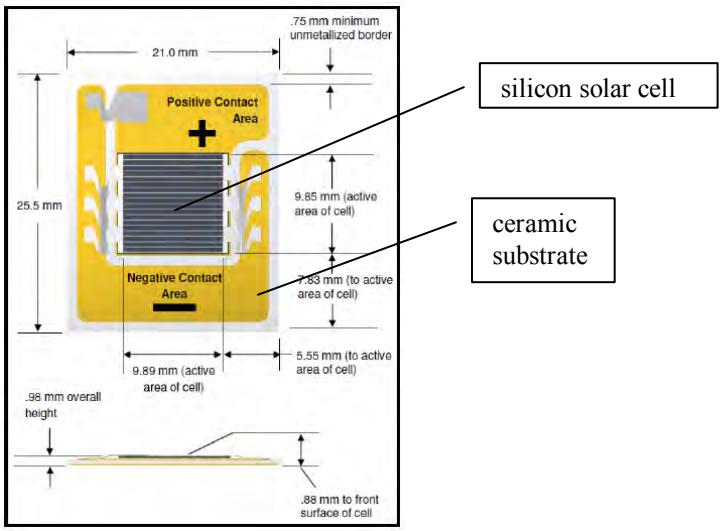

Figure 1. Detail of the solar cell model 100 CCA C3MJ 1 from Spectrolab-Boing, Source: Spectrolab

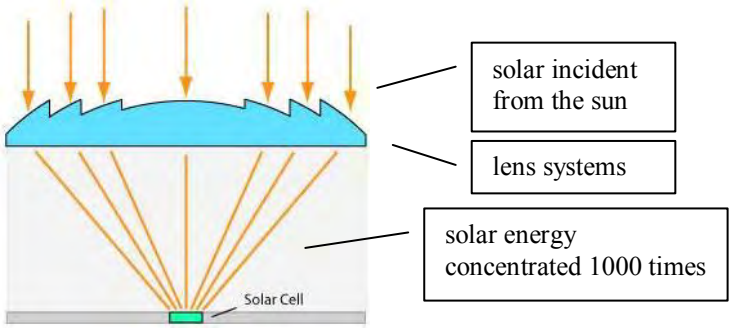

Figure 2. Concentration lens, Frenel model, on the PV cell. Source: www.greenrhinoenergy.com

Based on the dimensions of the HCPV cell from Spectrolab selected and presented previously in Figure 1, it is here proposed that our micro heat sink might be composed by a finned base and a top cover, both on copper with overall dimensions of 20 mm x 20 mm with a finned region dimensions of 10 mm x 10 mm, therefore approximately equal to the size of the silicon cell shown in this figure 1. To communicate the entrance and outlet of the microchannel is proposed a rectangular distributor located downstream and upstream of the microchannel as illustrated in Figure 5. Is noteworthy that the number of micro channels will be defined in the optimization step and therefore the seven channels shown in Figure 5 are for illustration only of the location and the type of heat exchanger that this work is proposed to design and optimize.

To ensure the structural integrity of the micro-heat exchanger the base and upper wall thickness was fixed in 100 micron. Due to limitations of the fabrication tools available at the time, the smallest channel width W_c, could be fabricated was 381μm and this value was then chosen and fixed as being the final width of the micro-channels. Thus in the optimization step the number of channels to be manufactured was determined by the optimized width of the fin wall, W_{fin}. The other two parameter that was optimized simultaneously was the channels height H_c, as illustrated in Figure 6, and the fluid flow rate U in which channel.

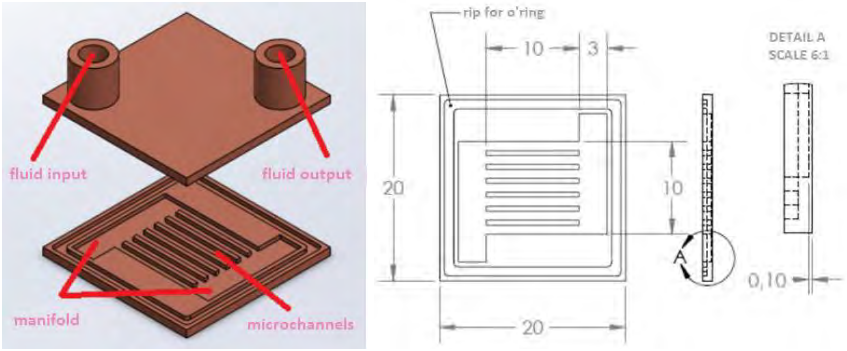

Figure 5. (a) Illustrative 3D view of the micro heat exchanger to be optimized. (b) Detailing of the main dimensions of the micro heat exchanger to be optimized.

ISSN 2176-5480

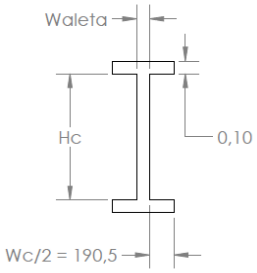

Figure 6. Geometrical parameters to be optimized, dimensions in µm.

3. OPTIMIZATION

Since the geometry and flow parameters to be optimized are defined (fin width, W_{fin}, channel height, H_c and fluid flow rate, U), the thermal and hydrodynamic simulation of the micro heat exchanger considering water as a Newtonian fluid, laminar flow, incompressible and viscous dissipation was developed in the commercial platform ANSYS CFX Workbench 14.5 using a Finite Volume Method for solving the 3D conjugated problem: continuity, momentum and thermal energy equations for the fluid domain and heat conduction equation for the solid domain in only one channel to reduce the computational cost of the problem, the boundary conditions employed for this simulated channel are illustrated in Figure 7 below.

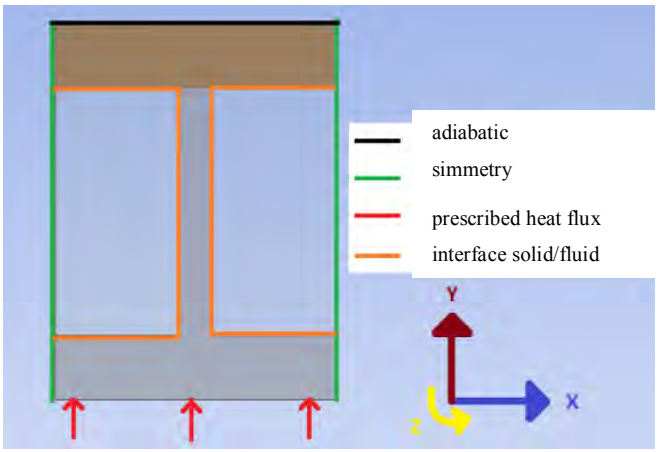

Figure 7. - Illustrative boundary conditions for one simulated channel.

In the optimization process, was used a interpolated response surface throw the Multi-Objective Genetic Algorithm - MOGA, respecting some restrictions and limitations such as, the average temperature of the solar cell, T_{cell}, should be less than 180 ºC by restriction of the manufactory of the photovoltaic cell; the non-uniformity of the solar cell temperature to increase the PV cell efficiency should be minimized through the monitoring of the standard deviation of the cell temperature, $\sigma_{T\text{cell}}$; Was considered a inlet fluid temperature of 60° C and desired that the outlet fluid temperature, T_s, should be between 80ºC and 90ºC; the maximum temperature in the hole fluid domain, T_{fMax}, should be less than 95°C, to avoid fluid change phase; the channel heigh,t H_c, was restricted to be between 0.5 e 2.5 times the channel width W_c., ie, between 190.5mm e 952.5 µm; despite the heat fins are desired to be thinner by limitations of structural strength and/or manufacturing step this is not always possible. Thus, the fin width, W_{fin}, in this design was restricted to vary between 50 e 381 µm; and the fluid flow rate, U, in the micro-channel was set to vary in a range from 50 and 250 mm/s. Table 1 below summarizes all this ranges and design constraints for the parameter to be optimized as well as the objectives to be achieved.

Table 1 summarizes the ranges of the parameters, design constraints and types of multi-objectives to be achieved.

	Symbol	Minimum value	Maximum value	Types of objective
Parameters	U (mm/s)	50	250	-
	W_{fin} (mm)	0.050	0.381	-
	H_c (mm)	0.1905	0.9525	-
Objectives	T_{cell} [K]	-	453.15	Minimize
	$\sigma_{T\text{cell}}$ [K]	-	-	Minimize
	T_s [K]	353.15	363.15	Maximize
	T_{fMax} [K]	-	368.15	Minimize

ISSN 2176-5480

The present work used a sparse grid mesh adaptive algorithm and hexahedral elements with a larger mesh refinement near the edges, Figure 8 illustrates the discretization used. A careful analysis of the convergence of the solution was carried out for different element sizes in the mesh, for the final results was used a mesh with elements of 12.5μm. Figures 9 to 12 illustrate the behavior of the four objective functions presented in table 1 in terms of the three parameters to be optimized, also presented in Table 1. In a general way, by the analysis of figures 9 and 12 it can be seen that the variable width of the fin, , W_{fin}, has a secondary role on the objective functions. The variables mean velocity of the fluid, U, and channel height, H_c, have a direct effect on the objective functions and are amplified when combined. As an example, by the analysis of Figure 9a, the increased thickness of the fin, W_{fin}, leads to a temperature increase of the cell, T_{cell}, considerably smaller than the effect of lowering the channel heigh, H_c. In figure 10c, on the other hand, the combined effect of the decrease in the mean flow velocity, U, and in the channel height, H_c, leading to a large increase in the standard deviation of the solar cell temperature, $\sigma_{T\text{cell}}$. Similar analyses to this may be made to the other figures.

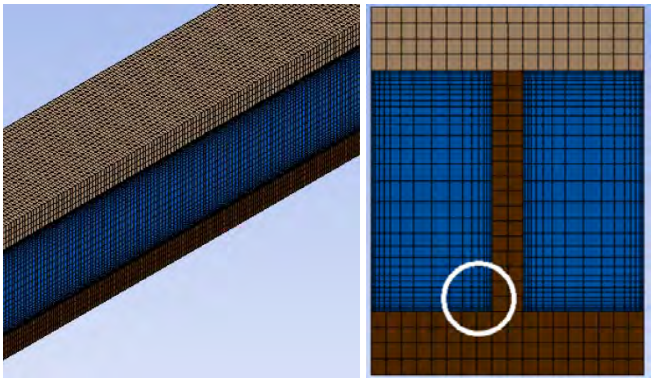

Figure 8. Illustration of the adaptative hexahedra elements employed in the discretization of domain

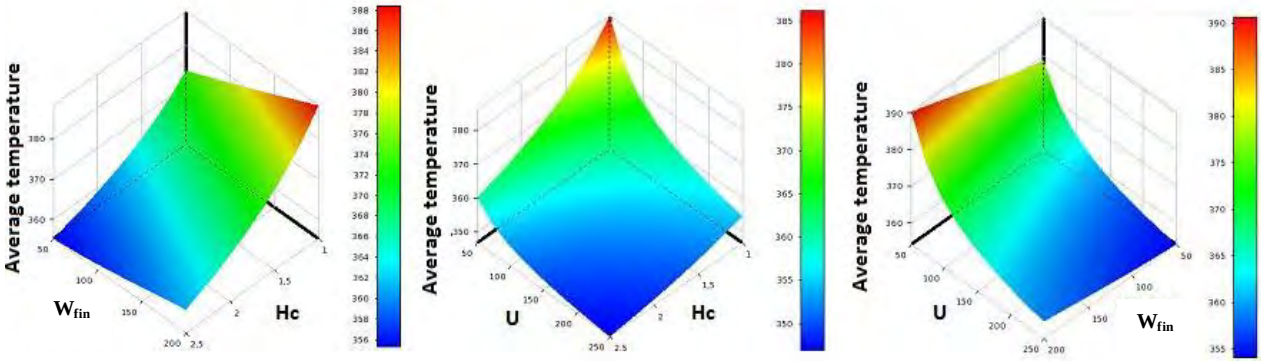

Figure 9. Response surface resulting from the optimization process – for the average solar cell temperature, T_{cell} [K]

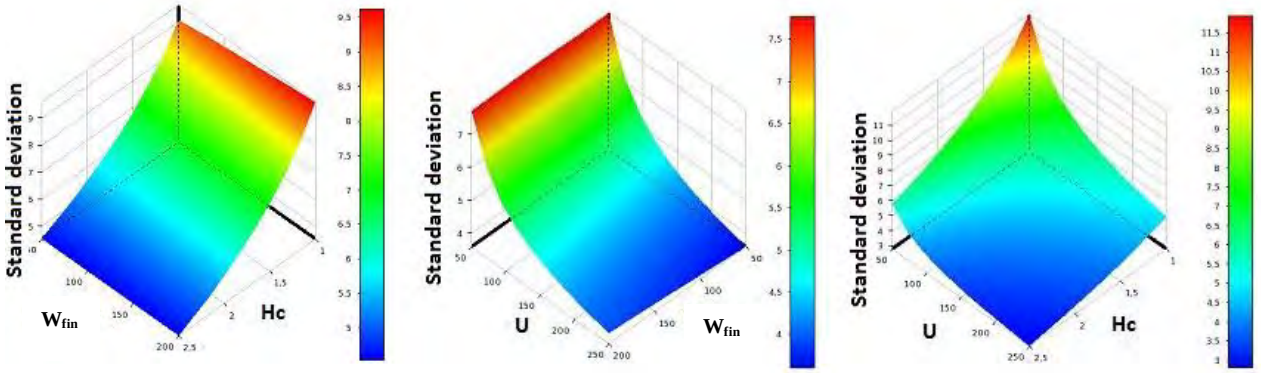

Figure 10. Response surface resulting from the optimization process – for the standard deviation of solar cell temperature $\sigma_{T\text{cell}}$ [K]

ISSN 2176-5480

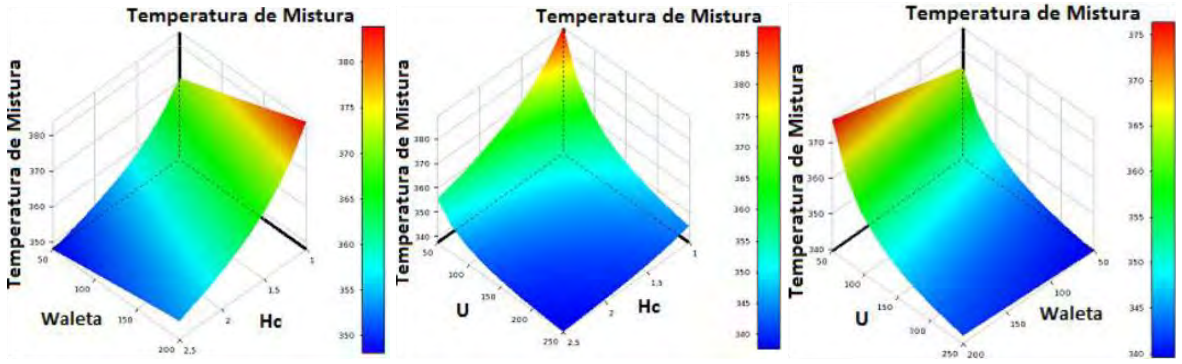

Figure 11. Response surface resulting from the optimization process – for the outlet fluid temperature domain, T_s[K]

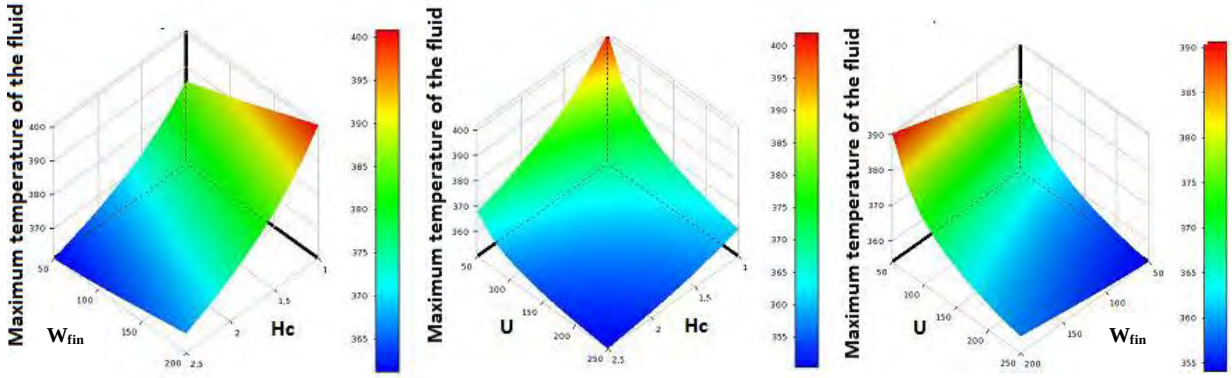

Figure 12. Response surface resulting from the optimization process – for the maximum temperature in the fluid domain, T_{fMax}[K]

In step optimization of geometric and hydrodynamic variables to achieve the objectives and design constraints was used the MOGA algorithm with 600 initial samples, 500 samples at each iteration a maximum percentage of Pareto admission of 75% and maximum number of iterations equal 15. The optimization process converged at the eleventh iteration, and the final optimized geometry is shown in Figure 13. Using this optimal dimensions presented in figure 13, the finned area of 10mmx10mm can be occupied with 17.7 micro-channels, so the fabricated micro-heat sink was made with 18 micro channels, and it's 3D isometric view can be seen in figure 13b.

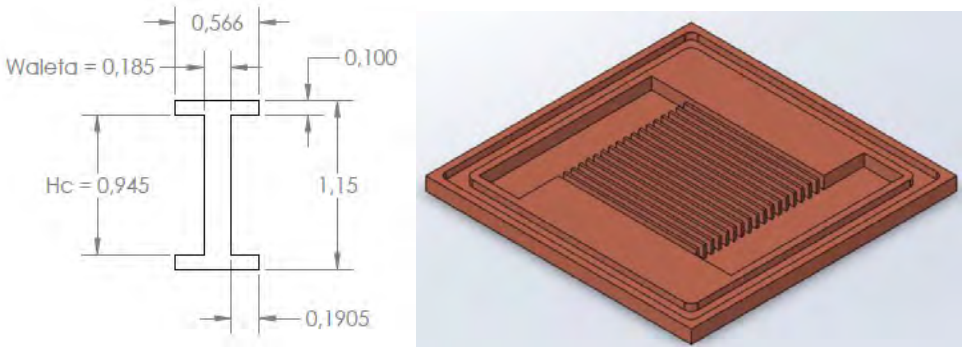

Figure 13. (a) Optimized geometry of which simulated channel; (b) 3D isometric view of the optimized micro-heat sink, with 18 micro-channels

Table 2 shows the minimum, average and maximum solar cell temperature obtained, as well as its standard deviation, for the hydrodynamic and thermal simulation of the single optimized micro-channel (Figure 13). In Table 2 is also possible to observe the hydrodynamic characteristics such as the Reynolds number, volumetric flow rate, pressure drop and power required for a single channel and also for the hole micro-heat exchanger, when disregarding the losses caused by the distribution channels. Figure 14 shows the temperature distribution for the fluid and the solid wall in the the inlet and outlet section of the micro channel, respectively. Analyzing the solid domain can be perceived a good temperature uniformity due to the high thermal conductivity of copper.

ISSN 2176-5480

Table 2. Thermal and hydrodynamic characteristics of the optimized channel

Thermal characteristics	Minimum substrate temperature [K]	351.98
	Average substrate temperature [K]	360.55
	Maximum substrate temperature [K]	366.45
	Standard deviation of temperature in the substrate [K]	4.57
	Maximum temperature of the fluid [K]	366.40
	Average temperature of the fluid [K]	353.01
Hydrodynamic characteristics in a microchannel	Reynolds number	45.4
	Flow [mm³/s]	26.9
	Pressure drop [Pa]	81
	Power required [W]	2.16×10^{-6}
Hydrodynamic characteristics in the micro-heat sink	Reynolds number	45.4
	Flow [mm³/s]	484.2
	Pressure drop [Pa]	81
	Power required [W]	3.89×10^{-5}

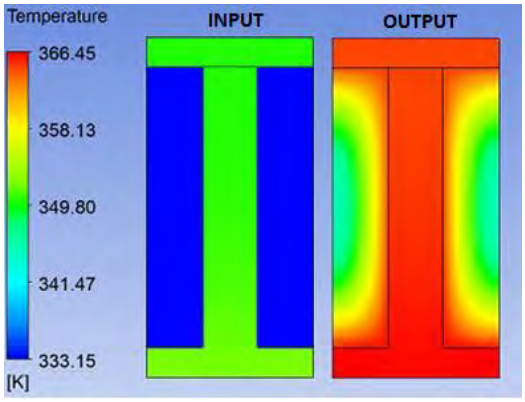

Figure 14. Temperature profile at the input and output channel

4. FABRICATION

In micro-milling step was used the Micro CNC Minitech Machinery, shown in Figure 15. The micro CNC has 4 motorized axis motor 4 is used, xyz and the function around xyz, which are fully controlled via a software. The maximum speed is 10,000 rpm and the displacement accuracy of 0.5 μm. For fixing the substrate to be machined in the micro-CNC there is two possibilities: with a traditional mechanical walrus or with a pneumatic one, using a vacuum pump, as can be seen in figure 15. The manufacturing was initiated by the base of the micro-heat exchanger that contains the input and output distributors and micro-channels, then the micro-heat exchanger cover was fabricated containing the connections for inlet and outlet.

Due to fabrication limitations and issues during this step, the optimized design of the machined micro-heat exchanger had to be slightly modified and the final dimensions are shown in Figure 16. The primary modification was with respect to the wall thickness of the base and cover that had been predicted to 100μm but have been manufactured with a thickness of 2.88 mm and 2.25 respectively. Figure 16. also shows in detail the type of connection to be used to the inlet and outlet in the micro-heat sink cover.

ISSN 2176-5480

The micro-milling procedure is started with the preparation and facing the substrate to be machined to assure perpendicularity between faces. Then the cutting parameters are set by the user (such as: feed rate in three directions-xyz, rotation speed of the tool, tool path, among others) through Visual Cad 2012 software that came with the micro-CNC. After defining the cutting parameters the software generates and program the sequence of cut that will be made, and then start the machining procedure. An incident jet of compressed air and a commercial Quimatic lubricant was used as a refrigerant during the machining procedure.

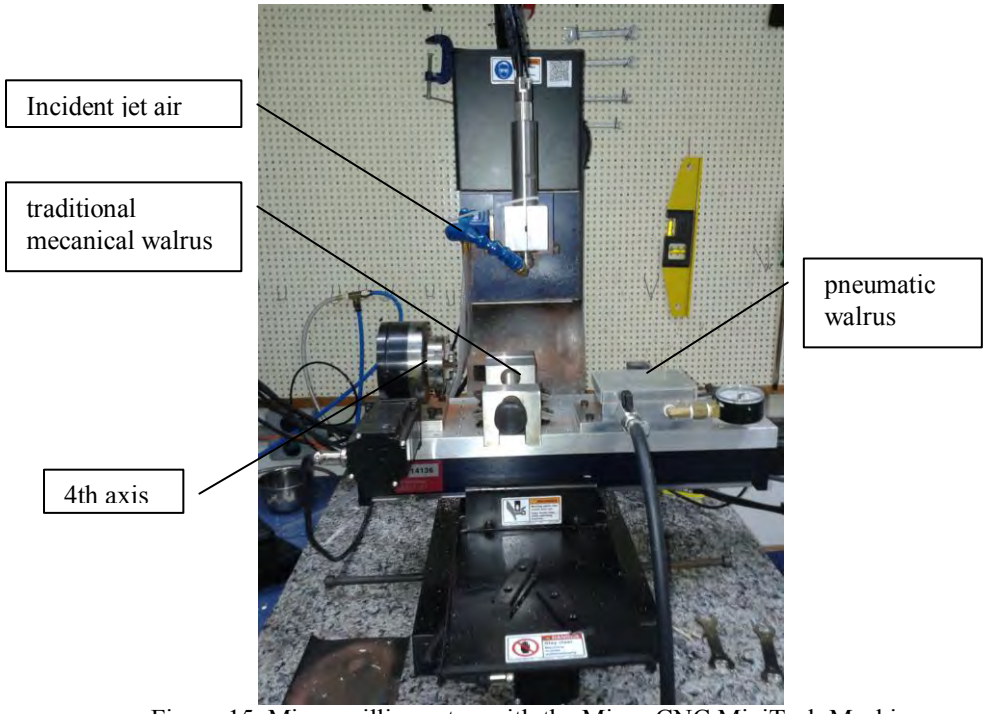

Figure 15. Micro-milling setup with the Micro-CNC MiniTech Machinery

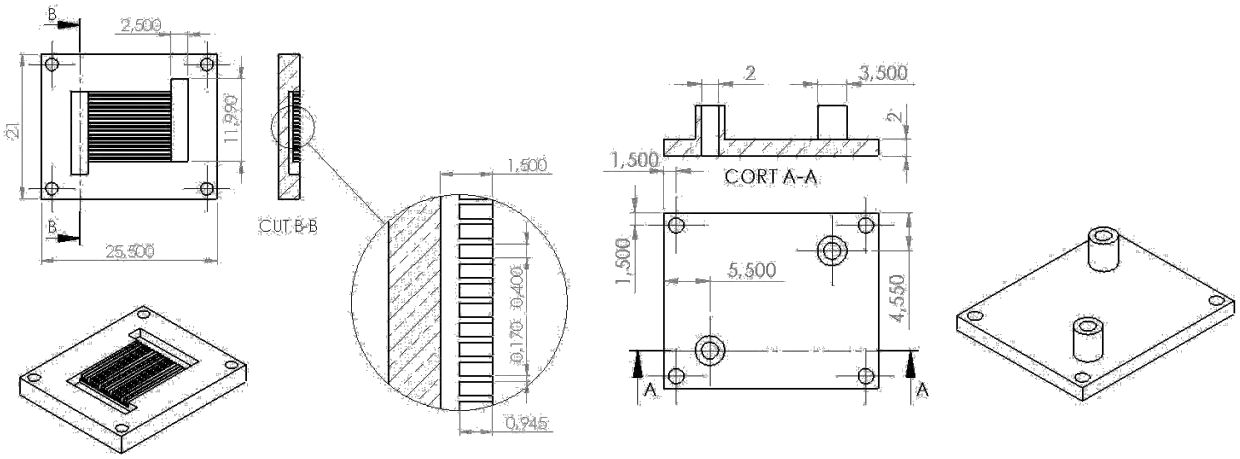

Figure 16. Technical drawing of the heat sink.

The manufacturing process of the micro-heat exchanger, detailed in Figure 16, was used a bar of 4inch. x ¼inch for the cover and a bar of a 1½inch x 1/8inch for the base. Using a cutting tool of 0.08 in (2.032 mm), both substrates were prepared and milled until it reaches the dimensions of 22.2mm x 21.2mm x 25.8mm for the cover and 2.87mm x 21.2mm x 25.8mm for the base. Then was used a cutting tool of 0.04inch (1,016 mm) for machining the distributors, and finally a cutting tool of 400 mm for machining the 18 micro-channels. Figure 17 illustrate the machining process of this micro-heat sink.

ISSN 2176-5480

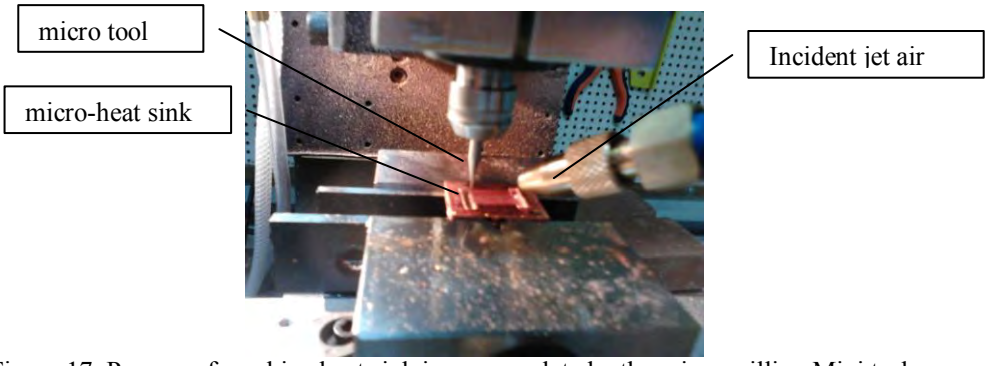

Figure 17. Process of machine heat sink in copper plate by the micro milling Mini tech.

The final internal and external dimension of the heat sink can be seen in Figure 18. Figures 18a to 18c show the microscopy and the final dimensions inside the micro-exchanger, showing in detail the inlet distributor, micro-channels and the outlet distributor, respectively. Figures 18d to 18f show images and the final dimensions of the external micro-exchanger, showing him before and after sealing.

In the micro- exchanger sealing, both surfaces of the base and cover, were polished with a 500 water sandpaper and then placed one over the other without any adhesive or O-ring between them. The attachment of the two part, cover and base, was made by four screws at the four edges of the micro-heat exchanger, as shown in Figure 16.

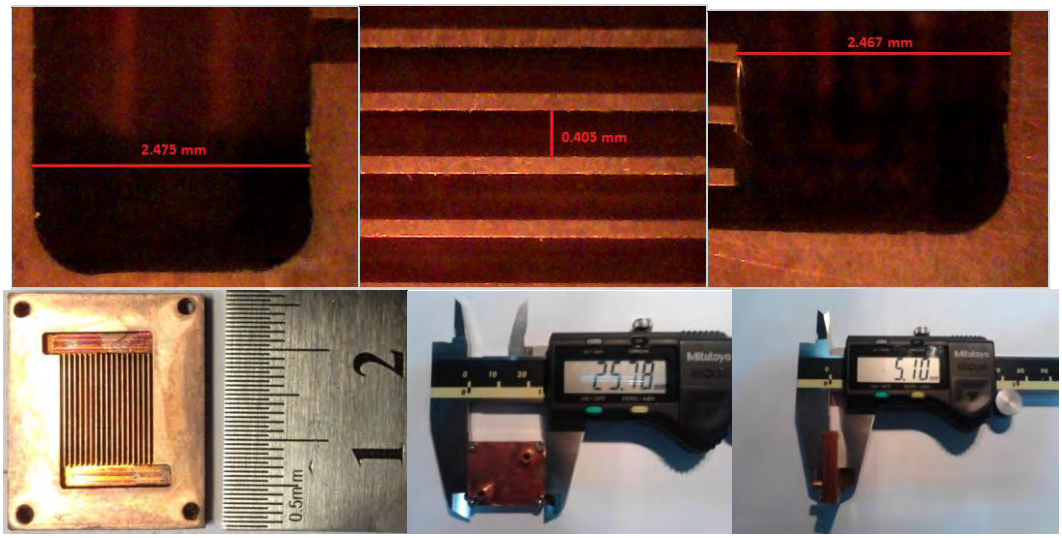

Figure 18. Final dimensions of heat sink

5. RESULTS AND DISCUSSION

In an experimental setup assembled specially for this study presented in Figure 19, the manufactured micro-heat exchanger was analyzed under controlled conditions. For the experimental measurements was used a infrared camera, Flir SC645, with microscopic lens and spatial resolution of 100μm, for a non-contact temperature measurements on the external surface of the micro-heat exchanger. Using an Agilent system, was made the acquisitions of measured temperatures from two thermocouples, located in the fluid mixture, respectively, at the inlet and outlet of the heat exchanger and from a third thermocouple measuring the ambient temperature. The heating of micro-heat exchanger was made by Joule effect through a resistance of 16Ω and 10mmx10mm and controlled by a voltage source. The infusion of the working fluid through the micro-heat exchanger was done using a syringe pump that can accurately controlled the flow rate.

The electrical resistance was positioned in the center of the micro-heat exchanger, below the finned base that containing the 18 micro-channel, in this assembly was used a thermal glue to reduction the thermal resistances and enhance the thermal contact. Below the resistance was used a rock wool cushion and followed by an acrylic plate to ensure thermal insulation and structural rigidity to facilitates the support of the whole set by two clamping jaws, as shown in detail in Figure 20a and schematically presented in Fig. 20b.

ISSN 2176-5480

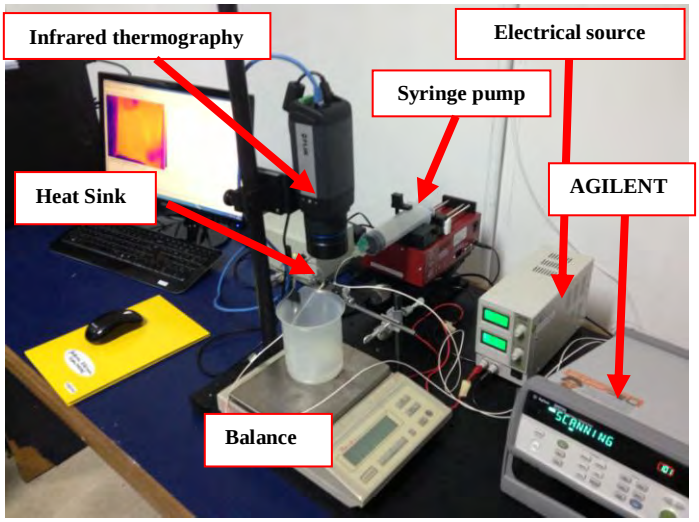

Figure 19. The experimental setup

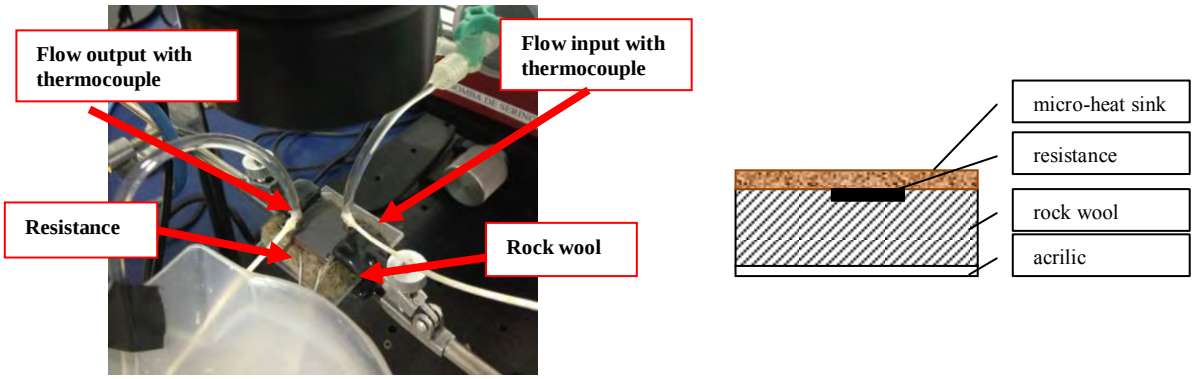

Figure 20. Heat sink instrumented

The experimental procedure is started by connecting the acquisition system (Agilen and IR camera) then the syringe pump is turned on in a previously determined flow rate, and then the electrical source is also turned on in a set voltage. The data acquisition is salved until the system reach steady state. Table 3 presents the three preliminary test cases conducted here with the fabricated micro-heat exchanger, for all three cases distilled water was used as the working fluid.

Table 3. Experimental cases

Case	Repeatability	Flow (mL/min)	Voltage (V)	Power (W)
1	3 x	10	10	6,25
2	3 x	10	12	9
3	3 x	10	14	12,25

Figure 21 shows the temperature variation average and the standard deviation of the fluid mixture between the outlet and the inlet of micro-heat exchanger along time, showing a good repeatability of the results for all cases, since can be observed a good graphic concordance of the results. For case 01 can observed an increase of 6.77 °C and a standard deviation of 0.057°C , for the case 2 can observed an increase of 9.788°C with a standard deviation of 0.064°C e for case 3 can observed an increase of 13.219°C with a standard deviation of 0.057°C.

Figure 22 presents an qualitative comparison through the IR image for three different times (1s, 10s, 100s) for all three cases. Where, 1s is a representative image of the initial condition, 10s a representative image of the beginning of the transient state and 100s is a representative image of the steady state.

ISSN 2176-5480

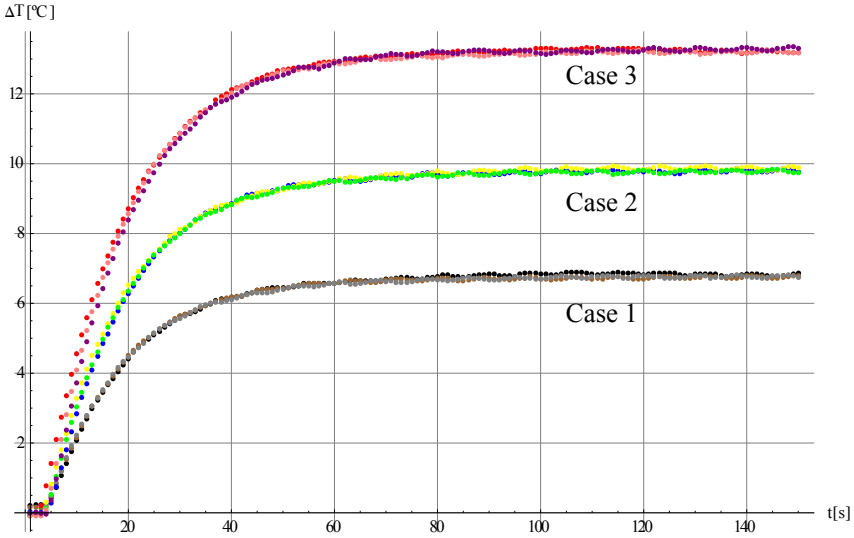

Figure 21. Repeatability analysis for case 2

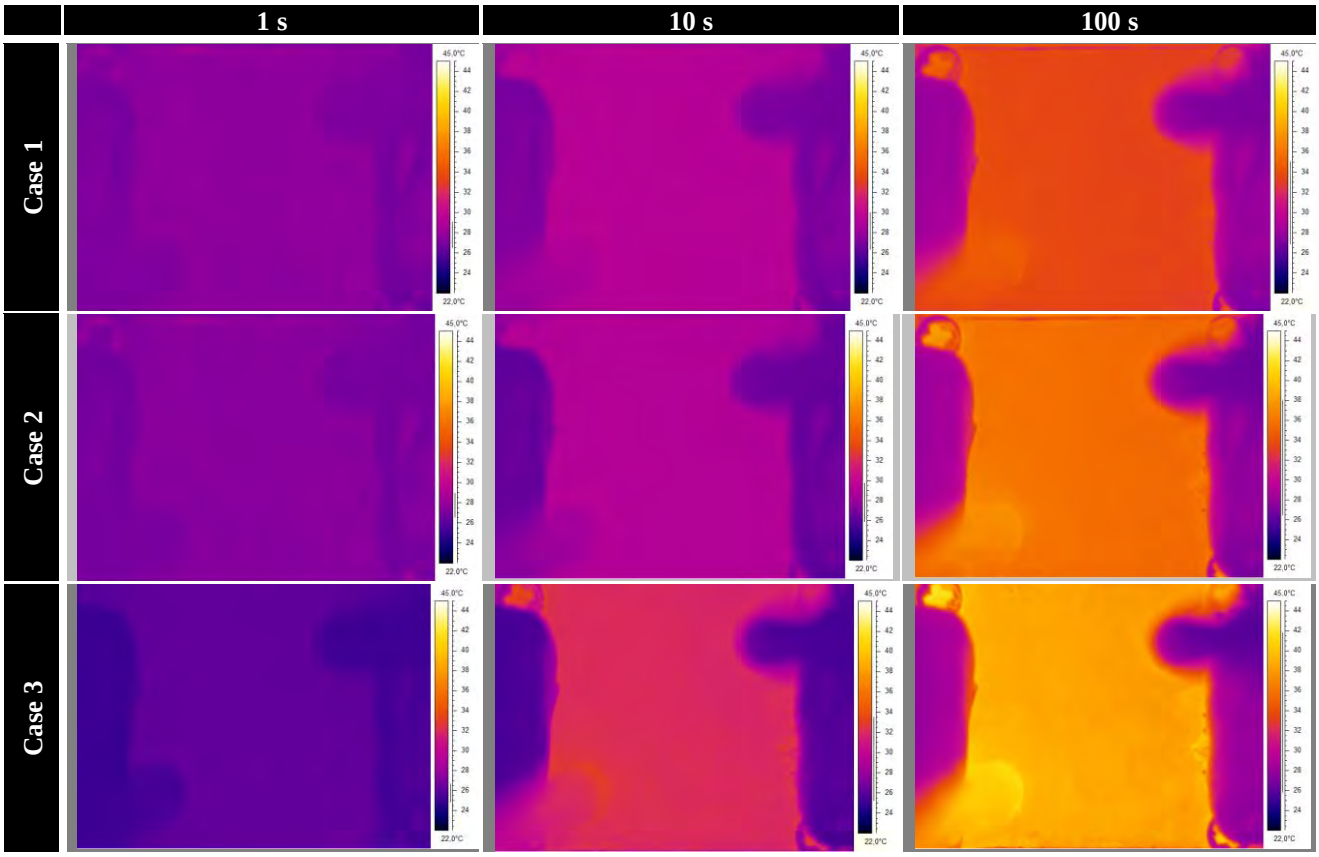

Figure 22. Imagens coletadas com a câmera termográfica para cada caso nos tempos: 1, 10 e 100 segundos

Table 4 shows some flow and heat transfer parameters calculated using experimental results for the three different cases presented in Table 3.

ISSN 2176-5480

Table 4. Global analysis

	Symbol	Case 1	Case 2	Case 3
Reynolds in which channel	Re	17.41	17.80	17.85
Total pressure drop in which channel	ΔP (Pa)	22.84	18.61	18.55
Hydraulic development length in which channel	L_h (mm)	0.802	0.819	0.822
Thermal development length in which channel	L_{Th} (mm)	2.99	2.98	2.98
Average mixture temperature between outlet and inlet	$\overline{T}$ (°C)	20.2	31.69	34.62
Total thermal load	$\dot{Q}$ (W)	4.74	6.79	9.20
Total power supplied by the electrical resistance	$\dot{Q}_{ELE}$(W)	6.25	9.0	12.25
Total heat losses by natural convection to the external air	$\dot{Q}_{air}$ (W)	0.000455	0.000626	0.000667
Thermal resistance of the heat sink	R_{th} (°C/W)	0.9289	1.0107	1.0170
Overall coefficient of the heat sink	U(W/°C.m^2)	10,765.5	9,893.65	9,832.31
Nusselt infinity in which channel	Nu_∞	5.69	6.57	7.05

6. CONCLUSIONS

This paper presents the optimized design, fabrication and experimental analysis of a heat sink based on micro-channels for efficient cooling of a commercial high concentration photovoltaic (HCPV) cell. The optimized geometry of the micro-heat sink was made using the platform ANSYS program Workbench 14.5 CFX and optimization tool Response Surface optimization, based on some requirements and design limitations such as: the mean temperature and standard deviation on the solar cell, the average fluid temperature at the micro-heat sink outlet and maximum temperature in the fluid domain. The micro-heat sink was manufactured in copper using a CNC-micro milling machine and an experimental setup was assembled to analysis the micro-heat exchanger first in laboratory conditions. The next step of this research is to carry out further experimental measurements in the laboratory with potential heating of micro-heat exchanger closer to what will be found when it is mounted photovoltaic panel HCPV.

7. ACKNOWLEDGEMENTS

The authors would like to acknowledge the partial financial support provided by the CNPq and FAPERJ.

8. REFERENCES

[1] T. HO, S. S. MAO and R. GREIF, "Improving efficiency of high-concentrator photovoltaic by cooling with two-phase forced convection," *International Journal of Energy Research,* pp. 1257-1271, 2010.

[2] T. HO, S. S. MAO e R. GREIF, "The impact of cooling on cell temperature and the practical solar concentration limits for photovoltaic," *International Journal of Energy Research,* 2010.

[3] A. ROYNE, C. J. DEY e D. R. MILLS, "Cooling of photovoltaic cells under concentrated illumination: a critical review," *Solar Energy Materials & Solar Cells,* pp. 451-483, 2005.

[4] G. SALA, "Cooling of solar cells," and *Cells and Optics for Photovoltaic Concentration*, Bristol, Adam Hillger, 1989, pp. 239-267.

[5] D. J. MBEWE, H. C. CARD e D. C. CARD, "A model of silicon cells for concentrator photovoltaic and photovoltaic thermal system design," *Solar Energy,* vol. 35, nº 3, pp. 247-258, 1985.

[6] V. L. DALAL e A. R. MOORE, "Design considerations for high-intensity solar cells," *Journal of Applied Physics,* vol. 48, nº 3, pp. 1244-1251, 1977.

[7] Sun Power, *Application notes for HED312 Silicon Concentrator Solar Cell,* 2002.

[8] R. W. SANDERSON, T. D. O'DONNELL e E. C. BACKUS, "The effects of non uniform illumination and temperature profiles on silicon solar cells under concentrated sunlight," and *14th IEEE Photovoltaic Specialists Conference*, 1980.

[9] E. KERMANI, *Manifold micro-channel cooling of photovoltaic cells for high efficiency solar energy conversion systems,* University of Maryland, 2008.

[10] B. D. TUCKERMAN e R. F. W. PEASE, "High-Performance Heat Sinking for VLSI," *IEEE Electron Device Letters,* vol. 2, nº 5, pp. 126-129, 1981.

ISSN 2176-5480

[11] M. A. EBADIAN e C. X. LIN, "A review of high-heat-flux heat removal technologies," *Journal of Heat Transfer,* vol. 133, nº 11, 2011.
[12] T. DANG e J. TENG, "Comparisons of the heat transfer and pressure drop of the micro channel and mini channel heat exchangers," *Heat and Mass Transfer,* vol. 47, nº 10, pp. 1311-1322, 2011.
[13] A. HUSAIN e K. KIM, "Optimization of a micro channel heat sink with temperature dependent fluid properties," *Applied Thermal Engineering,* vol. 28, nº 8-9, pp. 1101-1107, 2008.
[14] W. ESCHER, B. MICHEL e D. POULIKAKOS, "A novel high performance, ultra thin heat sink for electronics," *International Journal of Heat and Fluid Flow,* vol. 31, nº 4, pp. 586-598, 2010.
[15] Spectrolab, "CCA 100 C3MJ 1A Concentrator Cell Assembly," [Online]. Disponível em: http://www.spectrolab.com/DataSheets/PV/CPV/C3MJ_CCA-100_data_sheet.pdf. Acesso em 22 mar. 2013.

9. RESPONSIBILITY NOTICE

The authors are the only responsible for the printed material included in this paper.